Functionalized Metallic Single-Walled Carbon Nanotubes as a High-Performance Single-Molecule Organic Field Effect Transistor: An ab Initio Study

Hong Li,[†] Xin Yan,[†] Guangfu Luo,[†] Rui Qin,[†] Qihang Liu,[†] Lili Yu,[†] Chengyong Xu,[†] Jiaxin Zheng,[†] Jing Zhou,[†] Jing Lu,*[,†] Zhengxiang Gao,[†] Shigeru Nagase,[‡] and Wai Ning Mei[§]

State Key Laboratory of Mesoscopic Physics and Department of Physics, Peking University, Beijing 100871, People's Republic of China, Department of Theoretical Molecular Science, Institute for Molecular Science, Okazaki 444-8585, Japan, and Department of Physics, University of Nebraska at Omaha, Omaha, Nebraska 68182-0266

Received: July 14, 2010; Revised Manuscript Received: August 18, 2010

We propose a novel single-molecule organic field effect transistor (FET) fabricated via covalent functionalization of an individual metallic single-walled carbon nanotube (SWCNT). The transfer characteristic of this FET is calculated by using ab initio quantum transport calculations. Because of the significantly reduced screening effect of the quasi-one-dimensional electrode and seamless connection between the electrode and scattering region, the optimized device shows an excellent overall performance over the experimental single-molecule organic field effect transistors. This renders functionalized metallic SWCNTs a promising candidate for a high-performance single-molecule organic field effect transistor.

1. Introduction

Single-molecule organic field effect transistors (FETs) have a lot of fascinating characteristics, such as solution-processability, lightweight, possibility of large-area processing, low cost, flexibility, large carrier mobility, and quick device speed.[1] These charming characteristics earn them promising large-scale application in the future integrated circuit as basic elements. Significant progress has been made in the synthesis of sub-10-nm organic FETs in recent years.[2−8] Especially, the sub-10-nm-long organic FETs with metallic single-walled carbon nanotubes (SWCNTs) as quasi-1D source/drain (S/D) electrodes[2−5] usually exhibit better performance than those with bulky metal S/D electrodes.[6−8] The maximum on-state to off-state current ratio (I_{on}/I_{off} ratio) and minimum subthreshold swing (S) of the former FETs can reach to 10^5 and 400 mV/decade,[1,2,5] respectively, which is 3 orders of magnitude larger and 1 order of magnitude smaller, respectively, than those of the later FETs. The performance improvement of the former FETs is ascribed to the fact that the screening of the gate electric fields effect is much more insignificant in the SWCNT electrodes compared with the bulky metal electrodes.[5]

However, the experimental connections of the organic molecules and the metallic SWCNT electrodes are either covalent[3,5] or noncovalent.[2,4,5] There is a big Schottky barrier in the covalent connection, while electrons need to tunnel to conduct in the noncovalent connection. Both connections result in a small on-state current,[2−5] and a small on-state current implies a slow switching speed. One way to avoid a large contact resistance between the SWCNT electrodes and the scattering molecule is to construct an FET on an individual metallic SWCNT. Namely, the functionalized part of the SWCNT serves as a scattering region and the intact part as electrodes. Experimentally, such FETs have been fabricated by diazonium addition and acid oxidation, and the functionalized part is usually a few micrometers long.[9−12] In principle, we can construct a single-molecule FET by shortening the functionalized part of an individual metallic SWCNT to a few nanometers in length. Because of the seamless (or homogeneous) connection, the contact resistance is minimized and thus a larger on-state current and a higher switching speed than the present single-molecule FETs is highly expected in single-molecule functionalized-SWCNT-based FETs. However, the whole performance of single-molecule functionalized-SWCNT-based FETs is unknown.

In this article, we present an ab initio quantum transport study on the devices composed of sub-10-nm-long covalently functionalized armchair (5,5) SWCNTs seamlessly connected to pure metallic (5,5) SWCNT electrodes. Monovalent addition of phenyl (C_6H_5), triethylsilyl ($Si(CH_2CH_3)_3$), and methyl (CH_3) radicals and [2 + 2] cycloaddition of fluorinated olefin (perfluoro(5-methyl-3,6-dioxanon-1-ene) (PMDE)) are used to investigate the sp^3-type bonding to SWCNTs, whereas divalent addition of the dichlorocarbene (CCl_2) radical is applied to investigate the sp^2-type bonding to SWCNTs. Experimentally, diazonium (a analogue of phenyl),[9,12−14] $Si(CH_2CH_3)_3$,[15] CH_3,[16] PMDE,[17] and CCl_2[18,19] groups have been used to functionalize SWCNTs chiefly for the purpose of separating semiconducting and metallic SWCNTs.

2. Computational Details

A supercell with a size of 6.00 nm × 6.00 nm × 0.74 nm is constructed for C_6H_5, $Si(CH_2CH_3)_3$, CH_3, and CCl_2 addition to the infinite (5,5) SWCNTs, corresponding to three unit cells (60 C atoms) of the (5,5) SWCNT in the axial direction. A larger supercell with a size of 6.00 nm × 6.00 nm × 1.23 nm is constructed for PMDE addition, corresponding to five unit cells (100 C atoms) of the (5,5) SWCNT in the axial direction. We use the symbol (5,5)+$f(x)$ to denote the (5,5) SWCNT functionalized by an f radical with a coverage concentration of x (x is defined as ratio of the addition radical number to the carbon atom number in the (5,5) SWCNT). The maximum coverage concentration in our model is taken as x_{max} = 16.7% for the

* To whom correspondence should be addressed. E-mail: jinglu@pku.edu.cn.
[†] Peking University.
[‡] Institute for Molecular Science.
[§] University of Nebraska at Omaha.

10.1021/jp106535q
Published on Web 08/30/2010

smaller C_6H_5, CH_3, and CCl_2 groups and $x_{max} = 10.0\%$ and 4.0% for the larger $Si(CH_2CH_3)_3$ and PMDE groups, respectively. The steric hindrance prevents a higher x for both $Si(CH_2CH_3)_3$ and PMDE groups. The infinite functionalized (5,5) SWCNTs are then truncated to 2.21−8.86 nm in length and connected to the pure (5,5) SWCNT electrodes to form devices. All the infinite functionalized (5,5) SWCNTs are optimized within the density functional theory (DFT) by using an all-electron double numerical atomic orbital basis set (DN) as implemented in the DMol^3 package[20] with $1 \times 1 \times 3$ Monkhorst−Pack[21] k points. The convergence criterion of the maximum atomic force is 0.01 eV/Å. On the basis of the equilibrium structures, an all-electron double numerical atomic orbital basis set plus polarization function (DNP) and a $1 \times 1 \times 49$ Monkhorst−Pack[21] k-point grid are then used to calculate the electronic band structures.

The transfer characteristics of the functionalized (5,5) SWCNT devices are then calculated using the ATK 2008.10 code,[22,23] which is based on the DFT coupled with the nonequilibrium Green's function (NEGF) method. We use a mesh cutoff energy of 150 Ry and a single-ζ basis set (SZ). The electrode temperature is set as 300 K. The current is calculated using the Landauer−Büttiker formula[24]

$$I(V_{gate}, V_{bias}) = \frac{2e}{h}\int_{-\infty}^{+\infty}\{T_{V_{gate}}(E, V_{bias})[f_L(E - \mu_L) - f_R(E - \mu_R)]\}dE \quad (1)$$

where $T_{V\text{gate}}(E,V_{bias})$ is the transmission probability at a given gate voltage V_{gate} and bias voltage V_{bias}, $f_{L/R}$ is the Fermi−Dirac distribution function for the left/right electrode, and μ_L/μ_R is the electrochemical potential of the left/right electrode. In our model, we take the effect of gate voltage into account by adding a constant shift to the electrostatic potential of the scattering region. The generalized gradient approximation (GGA) of Perdew−Burke−Ernzerhof (PBE) form[25] is chosen for the exchange-correlation functional throughout the calculations.

As a test of the reliability of our method, we fabricate a two-probe model with one pentacene molecule noncovalently connected to the cutting (5,5) SWCNT with a gap (that is, channel length) of $L = 0.8$ nm. A typical p-type character with the off-state on $V_{gate} = 5.0$ V is obtained, as shown in Figure S1 of the Supporting Information. The I_{on}/I_{off} ratio, on-state current, and subthreshold swing are 92, 3.5 μS, and 2880 mV/decade, respectively, and the respective experimental values are $\sim 10^3$, $\sim 3.3 \times 10^{-2}$ μS, and 500 mV/decade in the pentacene nanocrystallite FET with SWCNT as electrodes and $L = 1-3$ nm. Note that the channel length in this experiment is about 3 times of the value in our theoretical model. If the channel length of our model increases by a factor of 3, we estimate that the I_{on}/I_{off} ratio will increase by a factor of a few to a few tens, whereas the on-state current will decrease by a factor of 2, and the subthreshold swing will decrease to 2740−1360 mV/decade according to our calculations (see below). This rough agreement between the theoretical and experimental field effects, especially the I_{on}/I_{off} ratio, inspires us. The larger deviation in the on-state current is attributed to the effects of impurity in the actual example, which always reduces the current.

3. Results and Discussion

A. Structure, Binding Energy, and Band Gap. An isolated phenyl can easily desorb and diffuse at room temperature on the surface of SWCNTs, and this desorption can be avoided

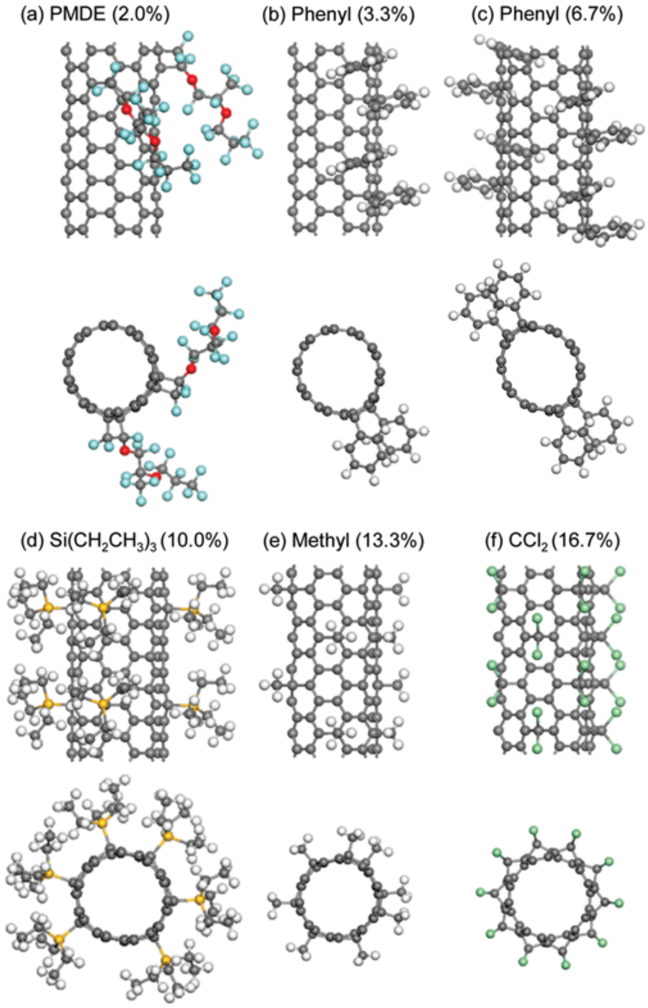

Figure 1. Side and top views of the typical optimized infinite functionalized (5,5) SWCNTs in the most stable adsorption configurations. Gray ball, C; white ball, H; yellow ball, Si; red ball, O; blue ball, F; green ball, Cl.

when two phenyls are paired because the binding energy per phenyl of paired phenyls is much larger than that of an isolated phenyl according to the calculations of Margine et al.[26] Consequently, only adsorption configurations with even radicals per supercell are considered in our model. Several adsorption configurations are considered for each radical at a given coverage concentration. The most stable adsorption configuration of the CCl_2 radical is taken from our previous calculation.[27] Typical optimized infinite functionalized (5,5) SWCNTs in the most stable adsorption configuration are shown in Figure 1, and the complete optimized structures in various adsorption configurations for each radical at a given coverage concentration are provided in Figure S2 of the Supporting Information. In general, the radicals of the sp^3-type bonding tend to pair, and those of the sp^2-type bonding always open the sidewall of the (5,5) SWCNTs in the most stable adsorption configuration. Both the structural characters of sp^3- and sp^2-type bonding are qualitatively similar to the previous studies.[26−36] We define binding energy per radical on the SWCNT as

$$E_b = (E(\text{tube} + n \times \text{radical}) - E(\text{tube}) - n \times E(\text{radical}))/n \quad (2)$$

where $E(\text{tube} + n \times \text{radical})$, $E(\text{tube})$, and $E(\text{radical})$ represent the total energy of the functionalized (5,5) SWCNT, pure (5,5)

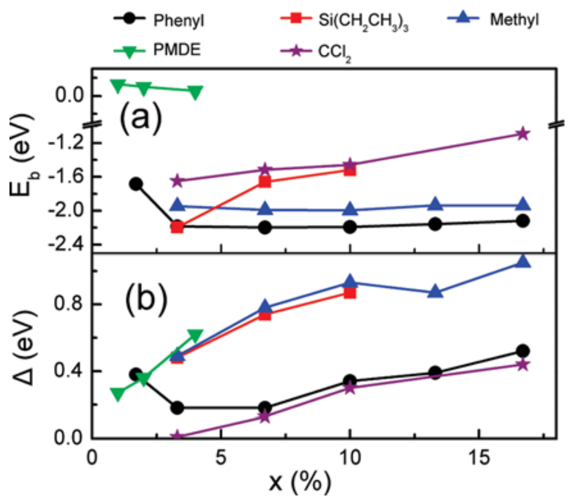

Figure 2. (a) Binding energy per radical and (b) band gaps of the infinite functionalized (5,5) SWCNTs in the most stable adsorption configurations as a function of the coverage concentration (x).

SWCNT, and radical, respectively, and n is the number of radicals per supercell. The calculated E_b values are given in Figure 2a; they are −1.09 to −1.65 eV for CCl_2, −2.12 to −2.20 eV for phenyl, −1.94 to −2.00 eV for methyl, −1.50 to −2.20 eV for $Si(CH_2CH_3)_3$, and 0.05−0.10 eV for PMDE. The addition of each radical is exothermic except for PMDE.

Chemical functionalization of the (5,5) SWCNTs causes a metal-to-semiconductor transition, and the band gaps (Δ) are generally increased with the increasing coverage concentration, as shown in Figure 2b. The metal-to-semiconductor transitions of SWCNTs induced by chemical functionalization have been previously reported.[27,29,31,33,35−37] The radicals can be classified into two groups according to the ability of opening a band gap. The first group covers three sp^3-type bonding $Si(CH_2CH_3)_3$, methyl, and PMDE, and the second covers sp^3-type bonding phenyl and sp^2-type bonding CCl_2. The radicals of the first group open a much larger band gap than those of the second group at a given coverage concentration. The complete band structures of the infinite functionalized (5,5) SWCNTs at various coverage concentrations in the most stable adsorption configurations are presented in Figure S3 of the Supporting Information.

B. Coverage Concentration Dependence of the Field Effects. Figure 3a shows a gated two-probe model constructed by an optimized ultrashort methyl-functionalized (5,5) SWCNT connected to the pure (5,5) SWCNT electrodes. The $I-V_{gate}$ curves at a bias voltage of V_{bias} = 0.02 V are calculated for phenyl, $Si(CH_2CH_3)_3$, methyl, PMDE, and CCl_2 radicals addition, respectively, as a function of the coverage concentration. The channel length is L = 2.21 nm for phenyl, $Si(CH_2CH_3)_3$, methyl, and CCl_2 addition, and L = 2.46 nm for PMDE addition. The calculated transfer characteristics are presented in Figure 3b−e, with the I_{on}/I_{off} ratios shown in Figure 4a. Bipolar gate effects are observed for phenyl and CCl_2 addition at $x \geq 10.0\%$, $Si(CH_2CH_3)_3$ and methyl addition at $x \geq 3.3\%$, and PMDE addition at $x \geq 2.0\%$. We ascribe the slight departure of the minimum leakage current from zero gate voltage to numerical error. Because the $I-V_{gate}$ curves are often asymmetric, the value of I_{on} is averaged over the I_{on} on the positive and negative V_{gate}. The I_{on}/I_{off} ratios are generally enhanced with x as a result of the increasing Δ. The increasing I_{on}/I_{off} ratio with reaction concentration has also been found in a-few-micrometers-long diazonium functionalized metallic SWCNT bipolar FET.[12]

Given a coverage concentration, the three radicals ($Si(CH_2CH_3)_3$, CH_3, and PMDE) that open a larger Δ also

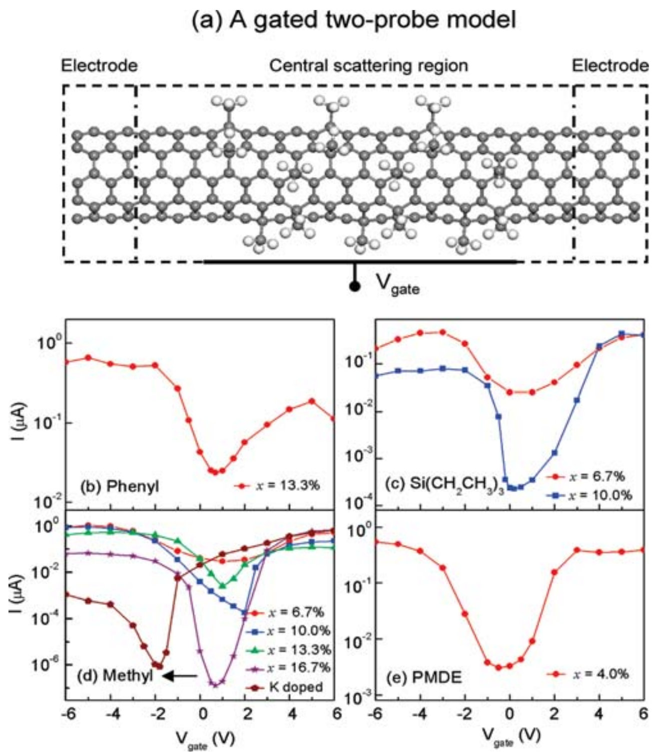

Figure 3. (a) A gated two-probe model constructed by an optimized ultrashort methyl-functionalized (5,5) SWCNT connected to the pure (5,5) SWCNT electrodes. The coverage concentration and the channel length of this model are x = 16.3% and L = 2.21 nm, respectively. Gray ball, C; white ball, H. (b−f) Calculated transfer characteristics (V_{bias} = 0.02 V) of the functionalized (5,5) SWCNT FETs as a function of the coverage concentration (x). The channel length is L = 2.21 nm for phenyl, $Si(CH_2CH_3)_3$, and methyl addition, and L = 2.46 nm for PMDE addition. Only the transfer characteristics with an I_{on}/I_{off} ratio > 10 are shown in this figure.

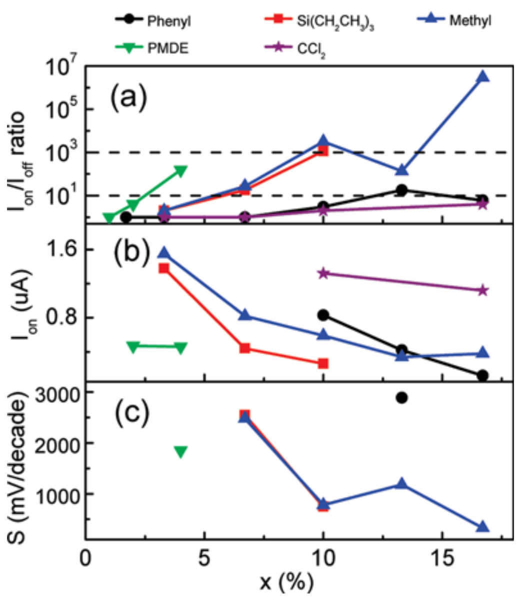

Figure 4. (a) I_{on}/I_{off} ratios, (b) on-state currents, and (c) subthreshold swings of the functionalized (5,5) SWCNT FETs at V_{bias} = 0.02 V as a function of the coverage concentration (x). The channel length is L = 2.21 nm for phenyl, $Si(CH_2CH_3)_3$, methyl, and CCl_2 addition, and L = 2.46 nm for PMDE addition.

generally have a larger I_{on}/I_{off} ratio than the two radicals (phenyl and CCl_2) that open a smaller Δ. The I_{on}/I_{off} ratios are quite similar between $Si(CH_2CH_3)_3$- and CH_3-functionlized SWCNT

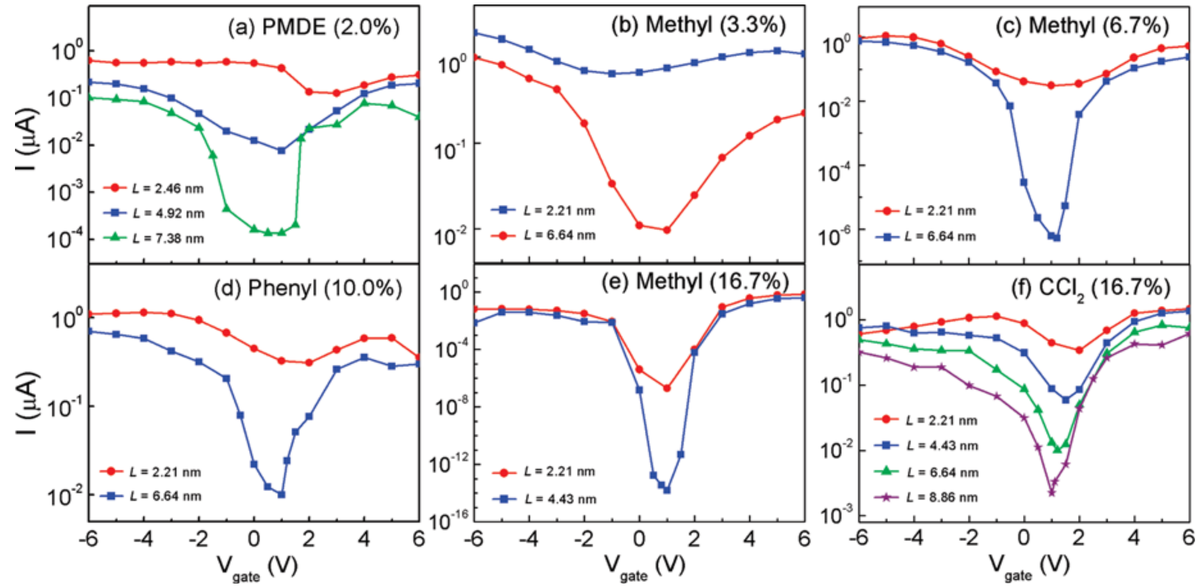

Figure 5. Calculated transfer characteristics (V_{bias} = 0.02 V) of the typical functionalized (5,5) SWCNT FETs as a function of the channel length (L).

FETs, and both of them are smaller than that of PMDE-functionalized SWCNT FETs at a similar x. Taken the coverage concentration and doping species dependence of the gate effects together, we conclude that a larger Δ opening of metallic SWCNTs generally results in a higher I_{on}/I_{off} ratio of the corresponding FET because the transmission coefficient of the off-state, and thus the leakage current, is generally reduced with the increasing Δ. The I_{on}/I_{off} ratios of the (5,5)+$Si(CH_2CH_3)_3$-(10.0%), (5,5)+methyl(10.0%), and (5,5)+methyl(16.7%) three FETs are over 10^3, and especially, the I_{on}/I_{off} ratio is up to over 10^6 in the (5,5)+methyl(16.7%) FET. The I_{on}/I_{off} ratio of a-few-micrometers-long diazonium functionalized metallic SWCNT bipolar FET is only 3.0 × 10^2.[12]

The on-state current determines the FET switching speed, whereas the off-state current determines the passive power consumed by a logic gate (e.g., an inverter). A high-speed low-power device should possess both a high I_{on}/I_{off} ratio and a high I_{on}.[38] The on-state currents I_{on} generally decrease with x, as shown in Figure 4b. For example, the I_{on} values decrease from 1.6 to 0.4 μA for the CH_3-functionalized (5,5) SWCNT FETs when x increases from 3.3% to 16.7%. The I_{on} values of $Si(CH_2CH_3)_3$-functionalized (5,5) SWCNT FETs are slightly smaller than those of the CH_3-functionalized (5,5) SWCNT FETs at a given x. When a larger bias voltage of V_{bias} = 0.50 V is applied to the (5,5)+methyl(16.7%) FET (see Figure S4 of the Supporting Information), the on-state current and conductance (G_{on}) are I_{on} = 4.0 μA and G_{on} = 8.0 μS, respectively. The experimental I_{on} of the sub-10-nm-long organic FETs with metallic SWCNT electrode is merely I_{on} = 3.0 × 10^{-2} to 5.0 × 10^{-2} μA and 5.0 × 10^{-7} to 2.0 × 10^{-2} μA for covalent[3,5] and noncovalent[2,4,5] connection modes between the electrode and scattering molecule at the same bias voltage, respectively. The experimental on-state conductance is G_{on} = 8.0 × 10^{-3} to 2.0 × 10^{-1} μS in the a-few-micrometers-long functionalized metallic SWCNT FETs.[9−12] Namely, the I_{on} in the (5,5)+methyl(16.7%) FET is 2 and 1 orders of magnitude higher than the maximum values in the sub-10-nm-long organic FET with a metallic SWCNT electrode and in the a-few-micrometers-long functionalized metallic SWCNT FETs, respectively.

The subthreshold swing (S) is also an important parameter of FETs. It determines how effectively the transistor can be turned off by changing the gate voltage. The S values of all the functionalized (5,5) SWCNT FETs with an I_{on}/I_{off} ratio > 10 are shown in Figure 4c as a function of x. (S here is defined as averaged $dV_g/d(\log I)$ over the value in the positive and negative V_{gate}). The subthreshold swings generally decrease with x. S decreases from 2480 to 330 mV/decade for the CH_3-functionalized (5,5) SWCNTs FETs when x increases from 6.7% to 16.7%, and the $Si(CH_2CH_3)_3$-functionalized (5,5) SWCNTs FETs have the same S at a given x. The minimum subthreshold swing experimental values obtained in the sub-10-nm-long organic FET is 400 mV/decade.[1,5] In one word, the (5,5)+methyl(16.7%) FET has the best overall performance among the checked functionalized (5,5) SWCNT FETs with an L of 2.21−2.46 nm, followed by the (5,5)+methyl(10.0%) and (5,5)+$Si(CH_2CH_3)_3$(10.0%) FETs. High coverage concentration of methyl on the (5,5) SWCNT is feasible because the binding energy per methyl is nearly unchanged from x = 3.3% to 16.7%.

C. Channel Length Dependence of the Field Effects. Next, we study the field effect change of the functionalized (5,5) SWCNT devices with the channel length. Typical transfer characteristics at V_{bias} = 0.02 V as a function of L are shown in Figure 5, and the corresponding I_{on}/I_{off} ratios are shown in Figure 6a. These I_{on}/I_{off} ratios monotonously increase with L. The I_{on}/I_{off} ratio of the (5,5)+methyl(6.7%) FET increases from 27 to 9.5 × 10^5 when L increases from 2.21 to 6.64 nm, much more quickly than those of the (5,5)+phenyl(10.0%), (5,5)+methyl(3.3%), (5,5)+CCl_2(16.7%), and (5,5)+PMDE(2.0%) FETs because the band gap of the former functionalized SWCNT (Δ = 0.78 eV) is larger than those of the latter four (Δ < 0.50 eV). Especially, the I_{on}/I_{off} ratio of the (5,5)+methyl(16.7%) FET increases from 2.9 × 10^6 to 1.4 × 10^{13} when L increases from 2.21 to 4.43 nm as it has the largest Δ of 1.05 eV. The I_{on}/I_{off} ratio of 1.4 × 10^{13} is extremely large, which is 4 orders of magnitude higher than the maximum experimental value obtained in nanoscale FETs,[39] and we are cautious about this result. Gate effects remain absent in the (5,5)+phenyl(3.3%) and (5,5)+phenyl(6.7%) devices even if L is increased to 11.07 nm because of a very small band gap of 0.18 eV for both of them. The increased I_{on}/I_{off} ratios with increasing L were also predicted for a-few-nanometers-long graphene nanoribbon (GNR) FETs[40−42] and a-few-ten-nanometers p-i-n SWCNT FETs.[43] Opposite results were reported experimentally in a-few-

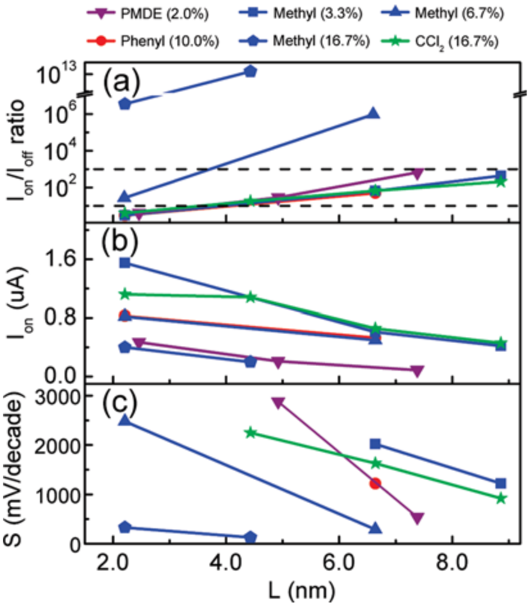

Figure 6. (a) I_{on}/I_{off} ratios, (b) on-state currents, and (c) subthreshold swings of the typical functionalized (5,5) SWCNT FETs at $V_{bias} = 0.02$ V as a function of the channel length (L).

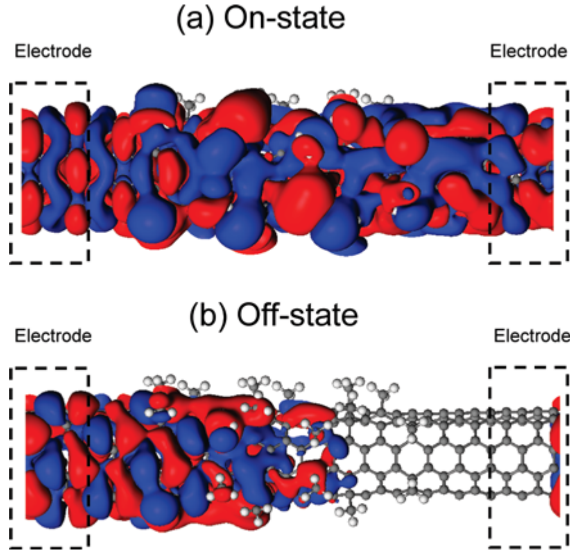

Figure 7. Transmission eigenchannels of the (5,5)+methyl(16.7%) FET with a channel length of $L = 2.21$ nm at the Fermi level for the (a) on- and (b) off-state. The isovalue is 10^{-2} a.u. Red and blue are used to indicate the positive and negative signs of the wave functions, respectively. Gray ball, C; white ball, H.

micrometers-long SWCNT FETs.[44] The increased I_{on}/I_{off} ratios with L in ultrashort SWCNT and GNR FETs[41−43] originates from the fact that the off-state current drops more rapidly with L than the on-state current because the tunneling probability of the off-state current decreases rapidly with L. Whereas the decreased I_{on}/I_{off} ratios with L found in long SWCNT FETs[44] is attributed to the prominent decrease of the on-state current caused by the increasing defect number on SWCNTs with L[44] and a slight rise of the off-state current with L.

The I_{on} values of all the examined devices decrease monotonously with L, as given in Figure 6b, due to the increasing number of scattering centers. For example, the I_{on} of the (5,5)+methyl(6.7%) FET decreases from 0.8 to 0.5 μA when L increases from 2.21 to 6.64 nm, and that of the (5,5)+methyl(16.7%) FET decreases from 0.4 to 0.2 μA when L increases from 2.21 to 4.43 nm. Experimentally, the I_{on} values of the pentacene FETs with SWCNT electrodes also decrease monotonously with L.[5] The S values decrease quickly with L, as displayed in Figure 6c. For example, S decreases from 2480 to 290 mV/decade for the (5,5)+methyl(6.7%) FET when L increases from 2.21 to 6.64 nm, and that of the (5,5)+methyl(16.7%) FET decreases from 330 to 130 mV/decade when L increases from 2.21 to 4.43 nm. The (5,5)+methyl(16.7%) FET with $L = 4.43$ nm has the best overall performance in all the checked devices, followed by the (5,5)+methyl(6.7%) FET with $L = 6.64$ nm and the (5,5)+methyl(16.7%) FET with $L = 2.21$ nm.

D. Discussions. From the above results, the group species, coverage concentration, and channel lengths are three key factors to determine the performance of single-molecule functionalized-SWCNT-based FETs. To obtain high-performance single-molecule functionalized-SWCNT-based FETs, the group capable of opening a large band gap of metallic SWCNTs, high doping concentration, and long channel is required. Methyl appears to be one of the best candidates because of its high ability of opening the band gap and allowable high doping concentration.

The transmission eigenchannels at the Fermi level (E_f) for the on- and off-state of (5,5)+methyl(16.7%) are given in Figure 7a and b, respectively. The transmission eigenvalue of the on-state is 0.85, which means that the incoming wave function is scattered little and contributes greatly to the conductance. Consistently, most of the incoming wave is able to reach to the other electrode. By contrast, the transmission eigenvalue of the off-state is 0.00, which means that the incoming wave function is totally scattered and does not contribute to the conductance. Consequently, the incoming wave is not able to reach to the other electrode at all.

Because as-made SWCNT FETs are always p-type, it is important to acquire n-type SWCNT FETs for the sake of application. We investigate whether an n-type SWCNT FET can be obtained by doping one K atom in the center of the (5,5)+methyl(16.7%) FET. The resulting transfer characteristic is shown in Figure 3d. The off-state moves from $V_{gate} = 0.7$ to -1.8 V, suggestive of a transition from bipolar behavior to an n-type one. The I_{on}/I_{off} ratio decreases from 2.9×10^6 to 8.0×10^5 because the leakage current increases, and meanwhile, the on-state current at the positive gate voltage is nearly unaffected by K doping. The maximum experimental I_{on}/I_{off} ratio obtained in the sub-10-nm-long p-type organic FET is 10^5.[1,2,5] The decrease in the I_{on}/I_{off} ratio is also predicted by Duan et al. in a GNR FET after N doping.[41] The subthreshold swing at the right side in the n-type (5,5)+methyl(16.7%) FET is 200 mV/decade, smaller than a value of 330 mV/decade in the undoped (5,5)+methyl(16.7%) FET.

A detailed comparison of the device characteristics between the theoretical high-performance sub-10-nm organic FETs from functionalized metallic (5,5) SWCNTs, the theoretical pentacene molecule FET, the experimental sub-10-nm organic FETs with metallic SWCNT electrodes,[2,5] and the theoretical sub-10-nm GNR FETs[41] is summarized in Table 1. The methyl-functionalized SWCNT FET with a high coverage concentration and long channel outperforms the experimental sub-10-nm organic FETs with metallic SWCNT electrodes in terms of I_{on}/I_{off} ratio, I_{on}, and S. It outperforms the GNR FETs by 10 orders of magnitude in terms of I_{on}/I_{off} ratio, competes with the latter in I_{on}, and has a larger S than the latter. The overall performance of the methyl-functionalized SWCNT FETs is also superior to that of the GNR FETs.

Finally, we suggest that sub-10-nm-long functionalized metallic SWCNT FETs can be fabricated following the same

TABLE 1: Comparison of Device Characteristics between the Theoretical High-Performance sub-10-nm Organic FETs from Functionalized Metallic (5,5) SWCNTs, the Experimental sub-10-nm Organic FETs with Metallic SWCNT Electrodes,[2,5] and the Theoretical sub-10-nm GNR FETs[41]

scattering molecule	connection type	type	x (%)	L (nm)	V_{bias} (V)	I_{on}/I_{off} ratio	I_{on} (μA)	G_{on} (μS)	S (mV/dec)
methyl-functionalized SWCNT (theoret)	seamless	bipolar	16.7	2.21	0.02	2.9×10^6	0.4	20.0	330
methyl-functionalized SWCNT (theoret)	seamless	bipolar	16.7	2.21	0.50	4.2×10^4	4.0	8.0	400
K-doped methyl-functionalized SWCNT (theoret)	seamless	n-type	16.7	2.21	0.02	8.0×10^5	0.7	35.0	200
methyl-functionalized SWCNT (theoret)	seamless	bipolar	16.7	4.43	0.02	1.4×10^{13}	0.2	10.0	130
methyl-functionalized SWCNT (theoret)	seamless	bipolar	6.7	6.64	0.02	9.5×10^5	0.5	25.0	290
$Si(CH_2CH_3)_3$-functionalized SWCNT (theoret)	seamless	bipolar	10.0	2.21	0.02	1.2×10^3	0.3	15.0	750
PMDE-functionalized SWCNT (theoret)	seamless	bipolar	2.0	7.38	0.02	6.6×10^2	9.0×10^{-2}	4.5	540
CCl_2-functionalized SWCNT (theoret)	seamless	bipolar	16.7	8.86	0.02	2.1×10^2	0.5	25.0	920
pentacene molecule (theoret)	noncovalent	p-type		0.80	0.02	0.9×10^2	7.0×10^{-2}	3.5	2880
pentacene nanocrystallite[5] (exptl)	noncovalent	p-type		1−3	0.60	$\sim 10^3$	$\sim 3.0 \times 10^{-2}$	$\sim 5.0 \times 10^{-2}$	∼500
poly-(3-hexylthiophene)[5] (exptl)	covalent	p-type		∼6.00	0.20	$\sim 10^4$	$\sim 2.0 \times 10^{-2}$	∼0.1	∼400
hexa-kata-benzoncoronene core layer[2](exptl)	noncovalent	p-type		∼3.00	−2.00	$\sim 10^5$	$\sim 2.0 \times 10^{-3}$	$\sim 1.0 \times 10^{-3}$	∼500
GNR[41] (theoret)	seamless	bipolar		5.91	0.02	$\sim 2.0 \times 10^3$	∼0.5	∼25.0	∼60
N-doped GNR[41] (theoret)	seamless	n-type		5.91	0.02	$\sim 3.0 \times 10^2$	∼0.6	∼30.0	∼200

procedure to fabricate other SWCNT FETs with a sub-10-nm-long channel.[2−5] To be specific, first, an individual metallic SWCNT is spin-coated with a blanket layer of PMMA, then a sub-10-nm-long window is opened on top of the metallic SWCNT by using ultra-high-resolution e-beam lithography, and, finally, the exposed part is functionalized through electrochemical modification,[9,11] simple immersion in the solution,[15] or plasma irradiation.[16]

4. Conclusion

We design a single-molecule FET by functionalization of an individual metallic SWCNT. Bipolar gate effects are observed for phenyl, $Si(CH_2CH_3)_3$, methyl, PMDE, and CCl_2 radicals. The I_{on}/I_{off} ratios generally increase with the increasing coverage concentration and channel length. The $Si(CH_2CH_3)_3$, methyl, and PMDE radicals generally have much more obvious gate effects than the phenyl and CCl_2 radicals at a comparable coverage concentration because they open a larger band gap of metallic SWCNTs. The optimized device has an I_{on}/I_{off} ratio and subthreshold swing of over 10^{13} and 130 mV/decade, respectively, and the corresponding on-state current is 2 orders of magnitude higher than the maximum experimental value of the sub-10-nm-long organic FETs. Thus, our investigation brings forward a novel method to construct high-performance single-molecule FETs by functionalization of metallic SWCNTs.

Acknowledgment. This work was supported by the NSFC (Grant Nos. 90206048, 20771010, 10774003, 90606023, and 20731160012), National 973 Projects (Nos. 2006CB932701, 2007AA03Z311, and 2007CB936200, MOST of China), Fundamental Research Funds for the Central Universities, the National Foundation for Fostering Talents of Basic Science (No. J0630311), the Program for New Century Excellent Talents in University of MOE of China, and the Nebraska Research Initiative (No. 4132050400) in the U.S.A. We thank Prof. Xuefeng Guo for helpful discussions.

Supporting Information Available: All the considered adsorption configurations of the optimized infinite functionalized (5,5) SWCNTs at various coverage concentrations, band structures of the optimized infinite functionalized (5,5) SWCNTs in the most stable adsorption configurations, the complete transfer characteristics of the functionalized (5,5) SWCNT FETs as a function of the coverage concentration at a bias voltage of V_{bias} = 0.02 V, transfer characteristics of (5,5)+methyl(16.7%) at a bias voltage of 0.5 V, and transfer characteristics of pentacene FET with (5,5) metallic SWCNT as electrodes. This material is available free of charge via the Internet at http://pubs.acs.org.

References and Notes

(1) Cao, Y.; Steigerwald, M. L.; Nuckolls, C.; Guo, X. F. *Adv. Mater.* **2010**, *22*, 20.
(2) Guo, X. F.; Myers, M.; Xiao, S. X.; Lefenfeld, M.; Steiner, R.; Tulevski, G. S.; Tang, J. Y.; Baumert, J.; Leibfarth, F.; Yardley, J. T.; Steigerwald, M. L.; Kim, P.; Nuckolls, C. *Proc. Natl. Acad. Sci. U.S.A.* **2006**, *103*, 11452.
(3) Guo, X. F.; Small, J. P.; Klare, J. E.; Wang, Y. L.; Purewal, M. S.; Tam, I. W.; Hong, B. H.; Caldwell, R.; Huang, L. M.; O'Brien, S.; Yan, J. M.; Breslow, R.; Wind, S. J.; Hone, J.; Kim, P.; Nuckolls, C. *Science* **2006**, *311*, 356.
(4) Guo, X. F.; Xiao, S. X.; Myers, M.; Miao, Q.; Steigerwald, M. L.; Nuckolls, C. *Proc. Natl. Acad. Sci. U.S.A.* **2009**, *106*, 691.
(5) Qi, P. F.; Javey, A.; Rolandi, M.; Wang, Q.; Yenilmez, E.; Dai, H. J. *J. Am. Chem. Soc.* **2004**, *126*, 11774.
(6) Cao, L. C.; Chen, S. Y.; Wei, D. C.; Liu, Y. Q.; Fu, L.; Yu, G.; Liu, H. M.; Liu, X. Y.; Wu, D. X. *J. Mater. Chem.* **2010**, *20*, 2305.
(7) Lee, J. B.; Chang, P. C.; Liddle, J. A.; Subramanian, V. *IEEE Trans. Electron Devices* **2005**, *52*, 1874.
(8) Wang, L.; Fine, D.; Jung, T. H.; Basu, D.; von Seggern, H.; Dodabalapur, A. *Appl. Phys. Lett.* **2004**, *85*, 1772.
(9) Balasubramanian, K.; Burghard, M.; Kern, K. *Phys. Chem. Chem. Phys.* **2008**, *10*, 2256.
(10) Goldsmith, B. R.; Coroneus, J. G.; Kane, A. A.; Weiss, G. A.; Collins, P. G. *Nano Lett.* **2008**, *8*, 189.
(11) Goldsmith, B. R.; Coroneus, J. G.; Khalap, V. R.; Kane, A. A.; Weiss, G. A.; Collins, P. G. *Science* **2007**, *315*, 77.
(12) Nguyen, K. T.; Shim, M. *J. Am. Chem. Soc.* **2009**, *131*, 7103.
(13) Strano, M. S.; Dyke, C. A.; Usrey, M. L.; Barone, P. W.; Allen, M. J.; Shan, H. W.; Kittrell, C.; Hauge, R. H.; Tour, J. M.; Smalley, R. E. *Science* **2003**, *301*, 1519.
(14) Wang, C. J.; Cao, Q.; Ozel, T.; Gaur, A.; Rogers, J. A.; Shim, M. *J. Am. Chem. Soc.* **2005**, *127*, 11460.
(15) Lee, Y.; Jeon, K. S.; Lim, H.; Shin, H. S.; Jin, S. M.; Byon, H. R.; Suh, Y. D.; Choi, H. C. *Small* **2009**, *5*, 1398.
(16) Zhang, G. Y.; Qi, P. F.; Wang, X. R.; Lu, Y. R.; Li, X. L.; Tu, R.; Bangsaruntip, S.; Mann, D.; Zhang, L.; Dai, H. J. *Science* **2006**, *314*, 974.
(17) Kanungo, M.; Lu, H.; Malliaras, G. G.; Blanchet, G. B. *Science* **2009**, *323*, 234.
(18) Hu, H.; Zhao, B.; Hamon, M. A.; Kamaras, K.; Itkis, M. E.; Haddon, R. C. *J. Am. Chem. Soc.* **2003**, *125*, 14893.
(19) Kamaras, K.; Itkis, M. E.; Hu, H.; Zhao, B.; Haddon, R. C. *Science* **2003**, *301*, 1501.
(20) Delley, B. *J. Chem. Phys.* **1990**, *92*, 508.
(21) Monkhorst, H. J.; Pack, J. D. *Phys. Rev. B* **1976**, *13*, 5188.
(22) Brandbyge, M.; Mozos, J. L.; Ordejon, P.; Taylor, J.; Stokbro, K. *Phys. Rev. B* **2002**, *65*, 165401.

(23) Taylor, J.; Guo, H.; Wang, J. *Phys. Rev. B* **2001**, *63*, 245407.
(24) Datta, S. *Electronic Transport in Mesoscopic Systems*; Cambridge University Press: Cambridge, England, 1995.
(25) Perdew, J. P.; Burke, K.; Ernzerhof, M. *Phys. Rev. Lett.* **1996**, *77*, 3865.
(26) Margine, E. R.; Bocquet, M. L.; Blase, X. *Nano Lett.* **2008**, *8*, 3315.
(27) Lu, J.; Wang, D.; Nagase, S.; Ni, M.; Zhang, X. W.; Maeda, Y.; Wakahara, T.; Nakahodo, T.; Tsuchiya, T.; Akasaka, T.; Gao, Z. X.; Yu, D. P.; Ye, H. Q.; Zhou, Y. S.; Meit, W. N. *J. Phys. Chem. B* **2006**, *110*, 5655.
(28) Ashraf, M. K.; Bruque, N. A.; Pandey, R. R.; Collins, P. G.; Lake, R. K. *Phys. Rev. B* **2009**, *79*, 115428.
(29) Chang, K.; Berber, S.; Tomanek, D. *Phys. Rev. Lett.* **2008**, *100*, 236102.
(30) Lee, Y. S.; Marzari, N. *Phys. Rev. Lett.* **2006**, *97*, 116801.
(31) Lee, Y. S.; Nardelli, M. B.; Marzari, N. *Phys. Rev. Lett.* **2005**, *95*, 076804.
(32) Lopez-Bezanilla, A.; Triozon, F.; Latil, S.; Blase, X.; Roche, S. *Nano Lett.* **2009**, *9*, 940.
(33) Park, H.; Zhao, J. J.; Lu, J. P. *Nanotechnology* **2005**, *16*, 635.
(34) Park, H.; Zhao, J. J.; Lu, J. P. *Nano Lett.* **2006**, *6*, 916.
(35) Song, C.; Xia, Y.; Zhao, M.; Liu, X.; Li, F.; Huang, B. *Chem. Phys. Lett.* **2005**, *415*, 183.
(36) Zhao, J. J.; Chen, Z. F.; Zhou, Z.; Park, H.; Schleyer, P. V.; Lu, J. P. *ChemPhysChem* **2005**, *6*, 598.
(37) Veloso, M. V.; Souza, A. G.; Mendes, J.; Fagan, S. B.; Mota, R. *Chem. Phys. Lett.* **2006**, *430*, 71.
(38) Nah, J.; Liu, E. S.; Varahramyan, K. M.; Shahrjerdi, D.; Banerjee, S. K.; Tutuc, E. *IEEE Trans. Electron Devices* **2005**, *57*, 491.
(39) Wu, P. C.; Ma, R. M.; Liu, C.; Sun, T.; Ye, Y.; Dai, L. *J. Mater. Chem.* **2009**, *19*, 2125.
(40) Huang, B.; Yan, Q.; Zhou, G.; Wu, J.; Gu, B.; Duan, W.; Liu, F. *Appl. Phys. Lett.* **2007**, *91*, 253122.
(41) Yan, Q. M.; Huang, B.; Yu, J.; Zheng, F. W.; Zang, J.; Wu, J.; Gu, B. L.; Liu, F.; Duan, W. H. *Nano Lett.* **2007**, *7*, 1469.
(42) Ouyang, Y.; Yoon, Y.; Guo, J. *IEEE Trans. Electron Devices* **2007**, *54*, 2223.
(43) Poli, S.; Reggiani, S.; Gnudi, A.; Gnani, E.; Baccarani, G. *IEEE Trans. Electron Devices* **2008**, *55*, 313.
(44) Aissa, B.; El Khakani, M. A. *Nanotechnology* **2009**, *20*, 175203.

JP106535Q